BIOCHEMISTRY
including biophysical chemistry & molecular biology

Article

pubs.acs.org/biochemistry

Molecular Level Interaction of Inositol Hexaphosphate with the C2B Domain of Human Synaptotagmin I

Meng-Je Joung, Sepuru K. Mohan, and Chin Yu*

Department of Chemistry, National Tsing Hua University, Hsinchu, Taiwan

ABSTRACT: Synaptotagmin I is a synaptic vesicle membrane protein that serves as a multifunctional regulator during the exocytosis of neurotransmitter release. It contains C2A and C2B domains. The binding of Ca^{2+} to the C2A domain activates the exocytosis of secretory vesicles, while the binding of inositol polyphosphates (IP4−IP6) to the C2B domain inhibits this process. To understand the IP6-induced inhibition of exocytosis of secretory vesicles, we determined the three-dimensional structure of the C2B−IP6 complex by nuclear magnetic resonance (NMR). In this study, we have determined the binding constant by isothermal titration calorimetry. The circular dichroism measurements demonstrated that IP6 can stabilize the C2B molecule. We identified the binding site using $^{1}H-^{15}N$ heteronuclear single-quantum coherence spectroscopy titration data and determined the structure of the C2B−IP6 complex using multidimensional NMR studies. This information will aid in the design of better pharmacological treatments for neurological disorders.

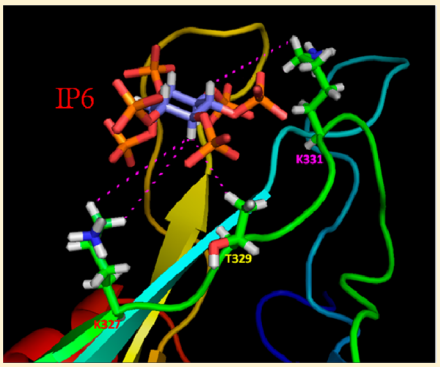

Synaptotagmins (Syts) make up a family of vesicle membrane proteins that includes more than 12 isoforms with diverse functions and tissue-specific expression patterns.[1,2] Syts all contain a short N-terminal intravesicular transmembrane region and tandem cytoplasmic repeats that are homologous to the C2 regulatory region of C2A and C2B.[3] Synaptotagmin I (Syt I), the best-characterized isoform, is expressed abundantly in neurons and is essential for fast Ca^{2+}-triggered neurotransmitter release.[4] The C2A domain of Syt I is considered to be a calcium sensor, because the binding between phospholipids and the C2A domain is Ca^{2+}-dependent.[5] The C2A domain also binds to syntaxin, a plasma membrane protein, in the presence of Ca^{2+}.[6,7] This interaction is necessary for exocytosis of neurotransmitter release.

Several proteins, such as clathrin assembly protein-2 (AP-2),[8] soluble NSF attachment protein (β-SNAP),[9] SNAP-25, and N-type calcium channels,[10−13] bind to different sites in the C2B domain. AP-2 is a multimeric protein complex that participates in cargo protein internalization during the clathrin-mediated endocytosis of synaptic vesicles on the plasma membrane. The interaction between the C2B domain and AP-2 was reported to play an important role in synaptic vesicle endocytosis. An in vivo study in *Caenorhabditis elegans* suggests that the C2B domain may function as a high-affinity docking site for AP-2 and serve as a bridge between endo- and exocytosis in the synaptic vesicle cycle.[14] It was also reported that the C2B domain binds inositol polyphosphates [IHPS, including inositol 1,3,4,5-tetrakisphosphate (IP4), inositol 1,3,4,5,6-pentakisphosphate (IP5), and inositol hexakisphosphate (IP6)] and phosphoinositide polyphosphates (PtdInsP*n*).[15−18] This binding is Ca^{2+} concentration-dependent. The binding module was determined using a liposome model system.[19]

IP6 is generally considered to be an antinutrient because of its ability to chelate divalent minerals and reduce the extent of their absorption.[20] IP6 was shown to inhibit free radical formation and weaken the lipid peroxidation catalyzed by iron and ascorbic acid in human erythrocytes.[20,21] A protective effect for IP6 was suggested because of its antioxidant effects and its ability to alter the cell signaling pathways that detoxify ROS (reactive oxygen species). A cell line assay using squid giant synapses indicated that the serial microinjection of IP6 into the presynaptic terminal inhibited synaptic transmission; this inhibition could be released by the co-injection of antibodies that recognize the C2B domain.[22] In addition, IP6 also plays an essential role in regulating the inhibition of neurotransmitter release, and this effect might partially be due to the inhibition of the interaction between Syt I and AP-2, which blocks endocytosis.[23]

The relationship between protein structure and function is important for the development of pharmacological agents for the treatment of human diseases. The C2B domain of Syt I is potentially involved in synaptic vesicle exocytosis. The aim of this study is to understand the interactions between C2B and IP6 at the molecular level. Here, we have used a variety of biophysical methods, including isothermal titration calorimetry (ITC), circular dichroism (CD) spectrometry, and multidimensional NMR, to characterize the interactions between C2B and IP6.

Received: January 2, 2012
Revised: March 8, 2012
Published: April 4, 2012

dx.doi.org/10.1021/bi300005w | *Biochemistry* 2012, 51, 3675−3683

MATERIALS AND METHODS

Reagents. GST-Sepharose was purchased from Amersham Pharmacia Biotech. $^{15}NH_4Cl$, ^{13}C-labeled glucose, and D_2O were purchased from Cambridge Isotope Laboratories. The components for the Luria broth media were obtained from AMRESCO. The Centricon and Amicon membranes were purchased from Millipore. All of the other chemicals used in the study were of high-quality analytical grade.

Protein Expression and Purification. The cDNA encoding the human C2B domain of Syt I (residues 270−421) was subcloned into the pGEX-4T1 expression vector. *Escherichia coli* cells expressing GST-tagged C2B were induced with isopropyl β-D-thiogalactopyranoside (IPTG) when the absorbance (at 600 nm) of the culture reached 0.6−0.9. The cells were harvested by centrifugation at 6000 rpm after being induced for 16 h at 25 °C. The unlabeled protein was expressed in Luria broth (LB) medium. The harvested cells were resuspended in resuspension buffer [50 mM Tris-HCl (pH 7.4) and 300 mM NaCl], and the cell walls were ruptured with a French press and via sonication. The cell lysate was centrifuged at 16000 rpm for 30 min. The supernatant was then incubated with glutathione Sepharose, and the resin was then extensively washed with resuspension buffer and 50 mM Tris (pH 7.4) containing 1 M NaCl to remove impurities. The bound GST−C2B protein was eluted with 10 mM glutathione in cleavage buffer [50 mM Tris, 0.1 M NaCl, and 2.5 mM $CaCl_2$ (pH 8.0)]. Thrombin cleavage was performed (2 NIH units/mL) at 25 °C for 20−24 h. Then, the whole solution was concentrated by Amicon and further purified by gel filtration on a Superdex 75 (Pharmacia) column using an FPLC system with 20 mM MES (pH 6.0) containing 150 mM NaCl and 2 mM DTT as the eluent. The purity of the protein was checked by sodium dodecyl sulfate−polyacrylamide gel electrophoresis, and its molecular weight was confirmed by electrospray mass analysis. The complete removal of nucleotide contaminants was verified by recording the UV spectrum of the protein.

Preparation of ^{15}N- and ^{13}C-Labeled C2B. Uniform labeling of the C2B domain using isotopes ^{15}N and ^{13}C was achieved by growth in M9 minimal medium. This medium contained either $^{15}NH_4Cl$ for single (^{15}N) labeling or $^{15}NH_4Cl$ and [^{13}C]glucose for double (^{15}N and ^{13}C) labeling of the C2B domain. The maximal expression yield was achieved using a modified M9 medium that included additional vitamins. The host expression strain, *E. coli* BL21(DE3), is a vitamin B1-deficient host, and therefore, thiamin (vitamin B1) was added to achieve yields of up to 10−15 mg of protein per liter from cells grown in the isotope-enriched medium.

Isothermal Titration Calorimetry (ITC). Protein−ligand binding was characterized by measuring the heat changes during the titration of an interacting ligand into a protein solution using a Microcal VP titration calorimeter. C2B and IP6 solutions were centrifuged and degassed under vacuum before being used. Titrations were performed by injecting 8 μL aliquots of IP6 (30 times, 1 mM) into a 0.1 mM C2B solution. The titrations were performed at 25 °C, with the protein and ligands dissolved in 20 mM MES (pH 6.0) containing 150 mM NaCl, 2 mM DTT, and 2 mM $CaCl_2$. The results of the titration curves were corrected using a buffer−protein control. Initially, the buffer alone was titrated, using IP6 as the ligand. Later, the same procedure was repeated with the protein dissolved in the buffer. The heat change of the first experiment (buffer titrated with IP6) was subtracted from that of the second (protein dissolved in buffer titrated with IP6), as shown in Figure 1. Finally, the Origin software supplied by Microcal was used to analyze these data.

CD Measurements. Circular dichroism measurements (CD) were taken using an AVIV CD spectrophotometer to determine the thermal stability of the protein. The thermal denaturation curves of the native free C2B domain and the C2B−IP6 complex were determined over a temperature range of 23−90 °C, at intervals of 3 °C for each data set, to determine the T_m of the protein in the presence and absence of the ligand. The protein sample was dissolved in 20 mM MES buffer (pH 6.0) containing 150 mM NaCl, 2 mM DTT, and 2 mM $CaCl_2$. The concentration of the protein sample was 10 μM, and the C2B−IP6 complex was present at a 1:1 C2B domain:IP6 ratio. The CD spectrum of the free C2B domain shows a positive ellipticity band at 228 nm, which is characteristic of a β-barrel protein, while the denatured protein does not produce a 228 nm CD band. The ΔG of unfolding was calculated from the slope of the folded and unfolded state baselines.

NMR Experiments. All of the two-dimensional (2D) and three-dimensional (3D) NMR resonance experiments were performed using a Varian 700 MHz NMR spectrometer equipped with a cold probe at 25 °C. The protein sample was present at 1.0 mM in a solution containing 20 mM MES (pH 6.0), 150 mM NaCl, 2 mM DTT, and 2 mM $CaCl_2$ in the presence of 10% D_2O. In a ^{13}C-filtered NOESY experiment, the spectra of the protein complex were recorded in 100% D_2O. The ^{15}N-labeled protein was titrated with IP6 at a 1:1 molar ratio in the binary complex. A plot of the weighted average of the ^{15}N and ^{1}H chemical shift perturbations of the protein residues was calculated using the equation $\Delta\delta = [(\delta^1H)^2 + 0.2(\delta^{15}N)^2]^{1/2}$. All of the spectra were processed using VNMR and analyzed using Sparky.[24]

3D NMR Experiments. The C2B resonances in the C2B−IP6 complex were assigned using various multidimensional NMR experiments. The backbone ^{1}H, ^{13}C, and ^{15}N resonances in the complex were assigned via 3D HNCA and HNCOCA experiments.[25] The side chain resonances were assigned using 3D ^{15}N-edited TOCSY-HSQC, HCCH-COSY, and HCCH-TOCSY data sets supplemented with data from other experiments, including CBCA(CO)NH[26] and HBHA(CO)-NH.[27] In addition, the C^α and C^β resonances were identified by CBCA(CO)NH experiments, and the carbon side chains of the protein binary complex were resolved by the CC(CO)NH experiment. HNCO spectra were used to assign the carbonyl carbons.[28] We also used the 3D ^{15}N-edited NOESY spectrum to identify the NH_2 groups of the amino acids Gln and Asn. The aromatic resonances of C2B were assigned using simultaneous ^{13}C- and ^{15}N-edited NOESY-HSQC spectra.[29] Intermolecular distance restraints were derived from the 3D ^{13}C, $^{15}N(F1)$-filtered, $^{13}C(F2)$-edited, and $^{12}C(F3)$-filtered NOESY-HSQC spectrum[30] of a 1:1 ^{15}N-, ^{13}C-, and ^{1}H-labeled C2B/IP6 (unlabeled) mixture.

Structure Calculation. The structure of the C2B complex was calculated iteratively using ARIA/CNS (version 2.2) with the PARALLHDG 5.3 force field in the PARALLHDG mode.[31] We used a variety of triple-resonance NMR experiments to determine the solution structure of C2B in the C2B−IP6 complex. Interproton distance restraints were derived from the NOE cross-peak intensities in the NOESY spectrum. In addition, hydrogen bond information was derived from a hydrogen−deuterium exchange experiment, and dihedral angle restraints were generated using TALOS[32] with the HN, CA,

dx.doi.org/10.1021/bi300005w | *Biochemistry* 2012, 51, 3675−3683

CB, CO, HA, and HB atoms. A total of 200 structures were calculated and further refined with CNS in an explicit solvent layer of water from which the best 16 structures with the lowest energies were selected. Here, we used PROCHECK to analyze the structure of the protein complex and extract its structural parameters.[33] MOLMOL and PYMOL were then used to generate structural representations.

Molecular Docking. The C2B−IP6 complex was assessed using HADDOCK (high-ambiguity-driven docking)[34−37] in combination with CNS.[38] The IP6 coordinates were taken from the Protein Data Bank (PDB) (entry 2K8R). The proton resonances of free IP6 were assigned using one-dimensional and 2D TOCSY and 2D NOESY, and the proton resonances of IP6 bound to C2B were assigned using an analysis of isotope-filtered TOCSY and isotope-filtered NOESY spectra.[39] The topology and the parameter files were generated using the HIC-UP server.[40] The docking procedure was driven by the intermolecular data derived from the 3D ^{13}C, $^{15}N(F1)$-filtered, $^{13}C(F2)$-edited, and $^{12}C(F3)$-filtered NOESY-HSQC data, which were used as restraints to dock IP6 with the ARIA/CNS-derived structure of the C2B domain. The intermolecular NOE data were used as unambiguous restraints, and the residues that showed chemical shift perturbations were used to define the ambiguous interaction restraints (AIRs) for each residue at the interface region as either active or passive. NACCESS[41] was used to identify the solvent-exposed residues in the C2B domain. Active residues had solvent surface accessible areas of >50%, while the passive residues had solvent surface accessible areas of <50%. The docking calculations were performed using HADDOCK 2.0, while the C2B domain (calculated from ARIA/CNS) and the IP6 parameters were optimized using PARALLELHDG, which included the optimized potentials for liquid simulation (OPLS) parameters for nonbonded interactions.[42] A total of 5000 structures were calculated, and the 50 structures obtained after water refinement were analyzed. The structures of the C2B−IP6 binary complex that were selected were the structures with the lowest-energy conformers.

RESULTS AND DISCUSSION

Syt I functions as a major Ca^{2+} sensor in neurotransmitter release through the binding of Ca^{2+} to its two C2 domains.[43,44] The two C2 domains have similar overall structures but different functions; binding of Ca^{2+} to the C2A domain serves a regulatory role in release, but binding of Ca^{2+} to the C2B domain is essential for release. However, it has been reported that IP6 strongly bound to the C2B domain and inhibited the fusion step of Ca^{2+}-regulated exocytosis.[45,46] Therefore, IP6 was assumed to be a potential regulator of neurotransmitter release. Thus, the elucidation of the structural interactions between the IP6 and C2B domains at the molecular level would provide the mechanistic information needed to understand how IP6 acts as an inhibitor of neurotransmitter release. In this study, we focused on determining the solution structure of the C2B−IP6 complex.

Isothermal Titration Calorimetry (ITC). The ITC technique measures the heat change associated with binding by simply titrating the ligand into a solution containing the macromolecule.[47] The heat changes are integrated and fit to obtain the full set of thermodynamic parameters of an interaction. Initially, injections of IP6 into the solution containing C2B domains produced strong heat changes. With progressive injections, the magnitude of the heat signal

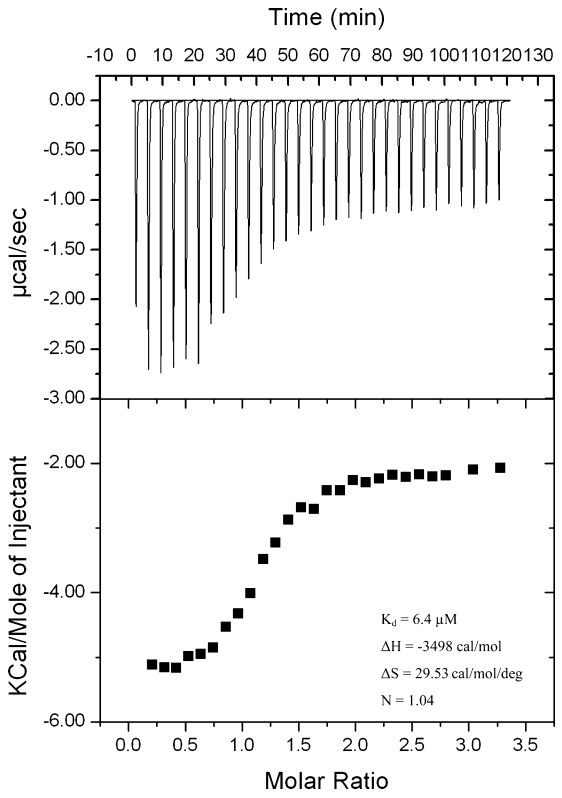

Figure 1. Isothermogram representing the binding of the C2B domain to IP6 at 25 °C. The binding constant of the C2B−IP6 interaction was 6.4 μM. The top panel shows the raw titration data, and the bottom panel shows the integrated heat changes after subtraction of the heat of dilution.

decreased as the IP6 binding sites of the C2B domains became saturated, until finally only the background heat of dilution was observed. The *N* value of the titration was 1.04, which indicated that IP6 had one binding site within the C2B domain (Figure 1). The equilibrium dissociation constant (K_d) of the protein−drug interaction was approximately 6.4 μM.

Chemical Shift Perturbation Experiments. The $^{1}H-^{15}N$ HSQC spectrum provides a fingerprint of the conformational state of a protein. The cross-peaks of the spectrum represent the chemical environment of the backbone and the side chain amides of the particular protein. Thus, the overlapping $^{1}H-^{15}N$ HSQC spectra of the free C2B domain and the C2B−IP6 binary complex provide information about the IP6-binding site within the C2B domain. Therefore, a comparison of the chemical shift perturbations ($\Delta\delta$) of the free and IP6-bound forms of the C2B domain is a useful method for identifying the C2B−IP6 binding interface.[48] The residues that show the highest chemical shift perturbation represent the binding region of IP6. Significant chemical shift perturbations were observed in the overlapping $^{1}H-^{15}N$ HSQC spectra of the free C2B domain and the C2B−IP6 complex at a 1:1 molar ratio (Figure 2A). The observed chemical shift perturbations of the bound form of the C2B domain might also appear as a result of a local conformational change that could be indirectly prompted by IP6 binding. At a 1:1 IP6:C2B domain titration ratio, several of the residues within the C2B domain showed chemical shift perturbations that were >0.1 ppm; however, residues K313, H315, L323, K325, K326, K327, G368, D371, K375, and V376 had the greatest chemical shift perturbations (Figure 2B). Residues displaying large chemical shift perturbations are

dx.doi.org/10.1021/bi300005w | *Biochemistry* 2012, 51, 3675−3683

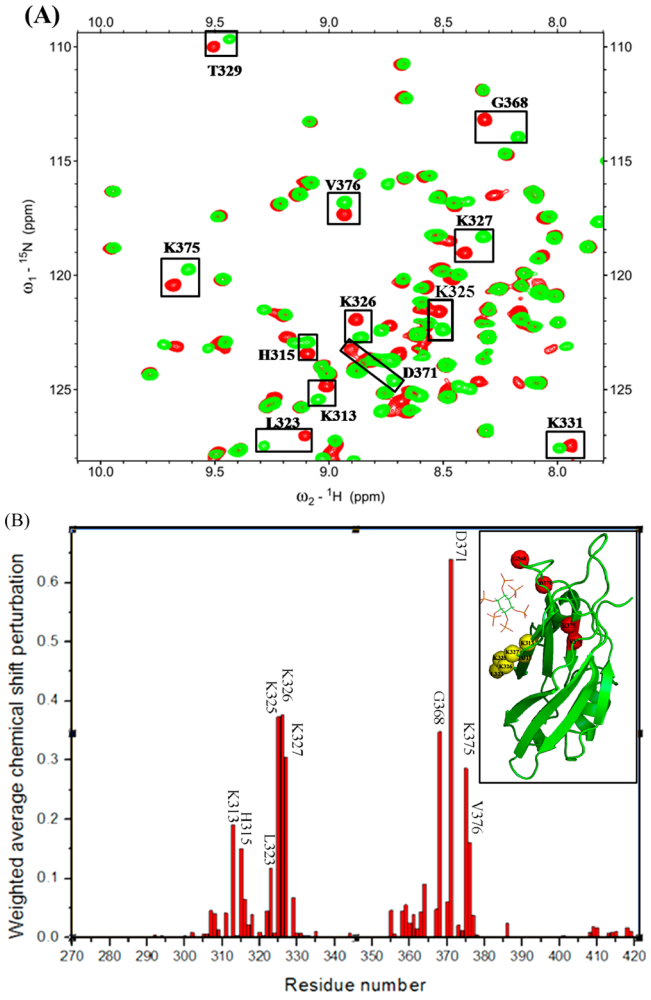

Figure 2. Analysis of the free C2B domain and the C2B–IP6 complex using 2D NMR at a 1:1 binding ratio. (A) The overlaid 2D $^{1}H-^{15}N$ HSQC spectra highlight the spectral changes in the uniformly ^{15}N-labeled C2B domain (green) and the C2B domain upon binding to IP6 (red). (B) Weight average of the chemical shift (^{1}H and ^{15}N) perturbations $\{\Delta\delta = [(\delta^{1}HN)^2 + 0.2(\delta^{15}N)^2]^{1/2}\}$ of the amino acid residues in the C2B domain upon complex formation with IP6. The inset depicts the significant chemically shifted residues mapped over the ribbon diagram of the C2B structure.

typically thought to indicate the putative binding region of the ligand. However, these pretreated residues were located in two distinct regions of the C2B domain (Figure 2B, inset). In Figure 2B, residues K313, H315, L323, and K325–K327 are colored yellow and G368, D371, K375, and V376 are colored red. IP6 was bound around these residues, except K375 and V376. These two perturbed residues (K375 and V376) might be chemically shifted because of secondary effects. It has been reported that point mutants in the polybasic Lys residues (K324–K327) within the C2B domain decrease the binding affinity of the C2B domain for IP6.[49] In addition, the ITC data suggest a one-binding site mode for the C2B–IP6 complex. To determine the exact binding region of IP6 on C2B, we determined the solution structure of the C2B–IP6 complex using intermolecular NOE data and chemical shift perturbation data.

The C2B Domain Is Stabilized by the Binding of IP6. The conformational changes that occur during the process of thermal denaturation in a protein can be determined by CD

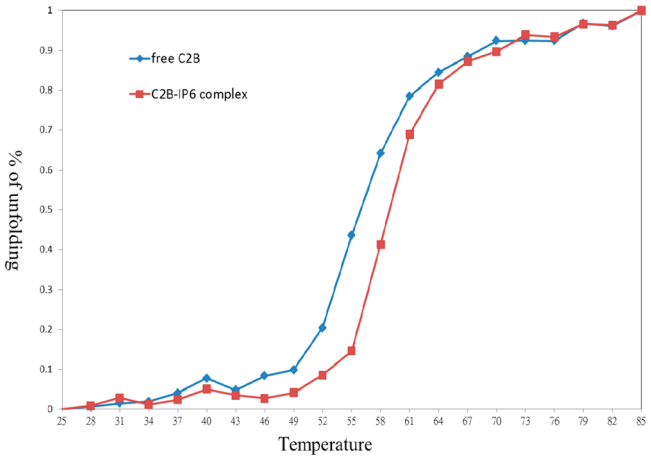

Figure 3. Analysis of the thermal stability of the C2B domain in the presence (■) and absence (◆) of IP6. Changes in the far UV-circular dichroism spectra were recorded by measurement of the ellipticity as a function of wavelength at 228 nm. The CD spectra were recorded in 20 mM MES buffer (pH 6.0) containing 150 mM NaCl, 2 mM DTT, and 2 mM $CaCl_2$ using a 1 mm cylindrical cuvette. The concentration of the protein sample was 10 μM, and the C2B–IP6 complex included a 1:1 C2B domain:IP6 ratio.

Table 1. Structural Statistics of the C2B Domain in the C2B–IP6 Complex from the ARIA/CNS Structure Calculation of the 20 Best Conformers

no. of distance constraints	
long-range	918
medium-range	411
short-range	462
intraresidue ($i = j$)	396
no. of dihedral angle constraints (φ/ψ)	110/110
no. of hydrogen bond constraints	60
no. of intermolecular NOEs	4
average rmsd from the mean structure (Å)	
residues 3–131	
backbone atoms	0.91 ± 0.12
heavy atoms	1.26 ± 0.11
regular secondary structure elements	
backbone atoms	0.56 ± 0.09
heavy atoms	1.06 ± 0.11
deviations from idealized geometry	
bond lengths (Å)	0.005 ± 0.001
bond angles (deg)	0.461 ± 0.056
impropers (deg)	0.585 ± 0.081
Procheck *G* factors	
dihedrals	−0.21
covalent	0.71
overall	0.03
Ramachandran statistics (% of all residues)	
most favored	85.0
additionally allowed	12.6
generously allowed	1.6
disallowed	0.8

spectroscopy. The thermal denaturation of both the free C2B domain and the IP6-bound form of the C2B domain was analyzed at temperatures ranging from 25 to 85 °C. The comparison and analysis of the CD data revealed that the melting temperature (T_m) of the C2B domain increased by 3 °C when it was bound to IP6 (Figure 3), as indicated by the

dx.doi.org/10.1021/bi300005w | *Biochemistry* 2012, 51, 3675–3683

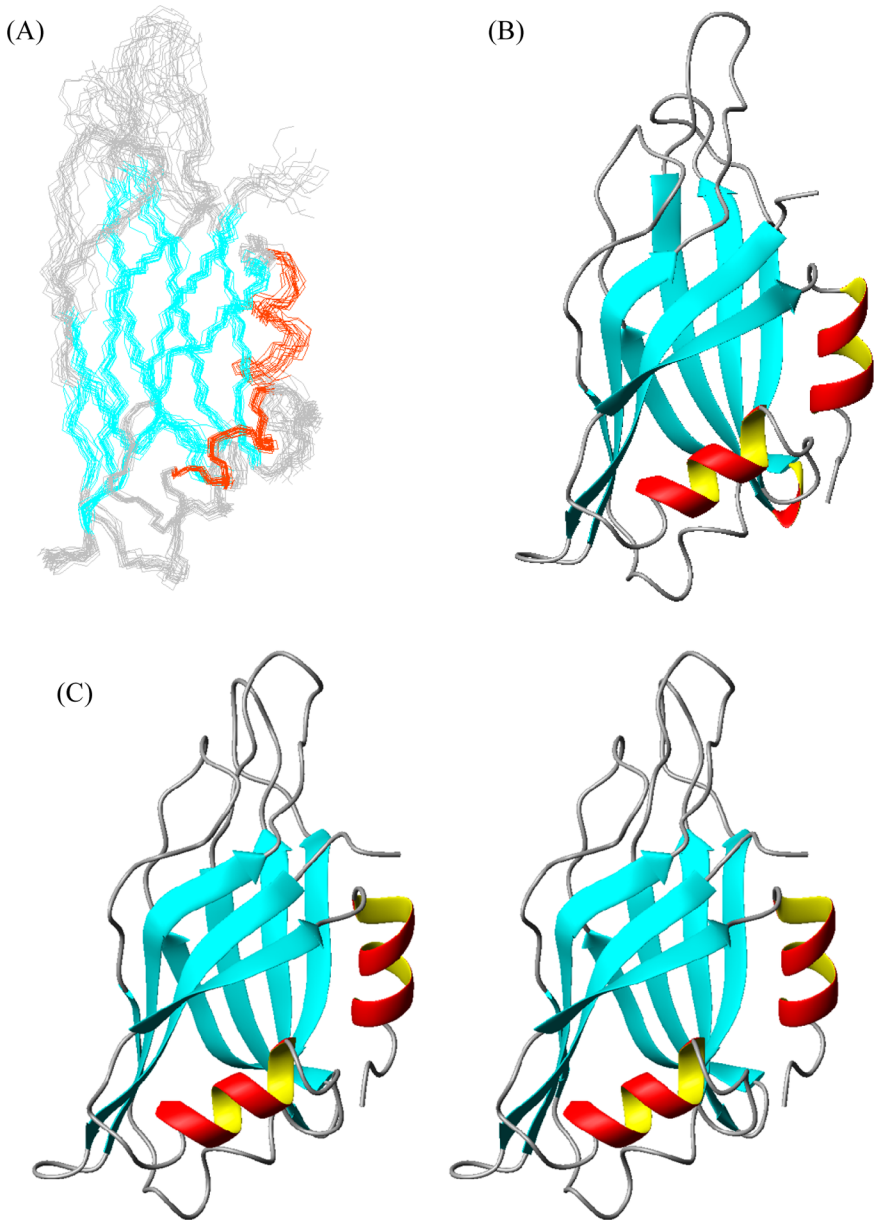

Figure 4. Solution structure of C2B in the C2B–IP6 complex. (A) Overlay of 16 structures showing the backbone representation of the C2B domain in the C2B–IP6 complex. The eight β-strands are colored cyan; the two α-helices are colored red, and the loop region is colored gray. (B) Ribbon representation of the C2B domain in the C2B–IP6 complex (average structure). (C) Stereopair showing C2B in the C2B–IP6 complex.

presence of a negative ellipticity band at 218 nm (characteristic of a protein possessing a β-barrel), indicating that IP6 stabilizes the C2B domain thermodynamically upon complex formation. The free energy of the C2B domain is 6.2 kcal/mol, and the free energy of the C2B domain in the C2B–IP6 complex is 8.4 kcal/mol. The unfolding free energy of the C2B domain increased by 2.2 kcal/mol in the presence of IP6.

Solution Structure of the C2B–IP6 Complex. We determined the solution structure of the C2B–IP6 protein complex using multidimensional NMR techniques. More than 95% of the ^{1}H, ^{15}N, C$^{\alpha}$, and C$^{\beta}$ chemical shifts were assigned in this set of analyses. The backbone of the C2B domain amide protons was assigned using the C2B ^{1}H–^{15}N HSQC resonance data (BMRB entry 5194). Because several residues were difficult to assign with the 2D HSQC, we followed up with HNCA and HN(CO)CA experiments to identify residues in the overall 2D ^{1}H–^{15}N HSQC spectrum. Distance restraints were subsequently generated from the ^{15}N-edited NOESY-HSQC and ^{13}C-edited NOESY-HSQC data and were used for the structure determination calculations. Hydrogen bond restraints derived from the hydrogen–deuterium exchange experiment were also used for structure determination. The structural restraints and statistics for the ensemble of the NMR structures calculated with ARIA/CNS are listed in Table 1. A total of 2187 NOEs were used for the calculation of the C2B–IP6 binary complex structure. The calculated structure of the C2B domain in the C2B–IP6 binary complex agrees well with the NMR structure of the free C2B domain (PDB entry 1K5W) in the structured region (two α-helices and eight β-sheets), with a backbone rmsd of 0.85 Å (Figure 4). According to a Ramachandran analysis, 85% of the residues were in the most favored region and <1% of the residues were in the disallowed region (Table 1).

dx.doi.org/10.1021/bi300005w | *Biochemistry* 2012, 51, 3675–3683

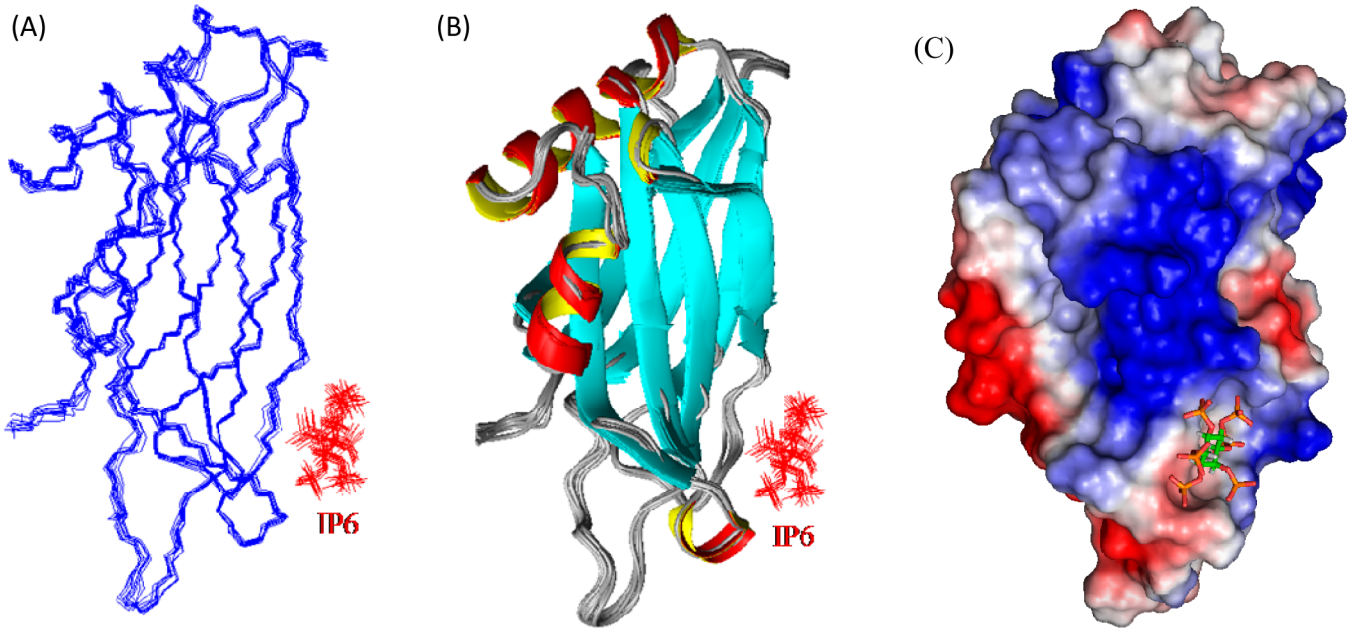

Figure 5. HADDOCK structure of the C2B−-IP6 complex. (A) Set of 10 overlapping structures representing the backbone of the C2B−IP6 complex. IP6 is colored red, and the C2B domain is colored blue. (B) Ribbon representation of the C2B−IP6 complex structure. IP6 is shown in ball-and-stick representation. (C) Surface representation of the C2B−IP6 complex.

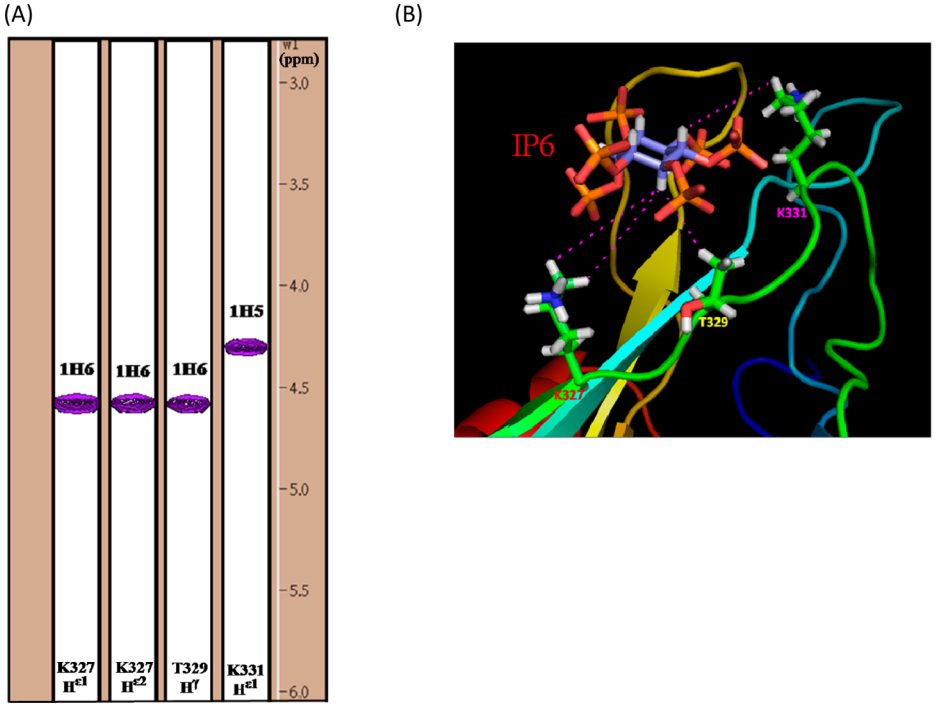

Figure 6. Intermolecular NOEs between the C2B domain and IP6. (A) Intermolecular NOE peaks of the C2B−IP6 complex determined from the 3D ^{13}C, $^{15}N(F1)$-filtered, $^{13}C(F2)$-edited, and $^{12}C(F3)$-filtered NOESY-HSQC data represented as strips. (B) Magnified view of the C2B−IP6 complex showing the binding region and the corresponding residues involved in the intermolecular NOEs indicated by pink dotted lines.

The C2B−IP6 binary complex was analyzed using HADDOCK (Figure 5). To determine the structure of the complex, we used the ^{13}C-filtered intermolecular NOEs and the chemical shift perturbation data as unambiguous and ambiguous data, respectively. The intermolecular NOEs indicated that four amino acid residues of the C2B domain interact with IP6 (Figure 6A). The four intermolecular NOEs between the C2B domain and IP6 are illustrated in Figure 6B. Residues K327, T329, and K331 in the C2B domain exhibited intermolecular NOEs with IP6. The ambiguous interaction restraints (AIRs) were subsequently defined for residues that showed a significant chemical shift perturbation in the 2D $^{1}H-^{15}N$ HSQC spectrum. The active residues for the HADDOCK calculations included residues K327, T329, and K331, and the group of passive residues included K313, H315, L323, K325, K326, L362, D363, Y364, I367, D371, K375, and

dx.doi.org/10.1021/bi300005w | *Biochemistry* 2012, 51, 3675−3683

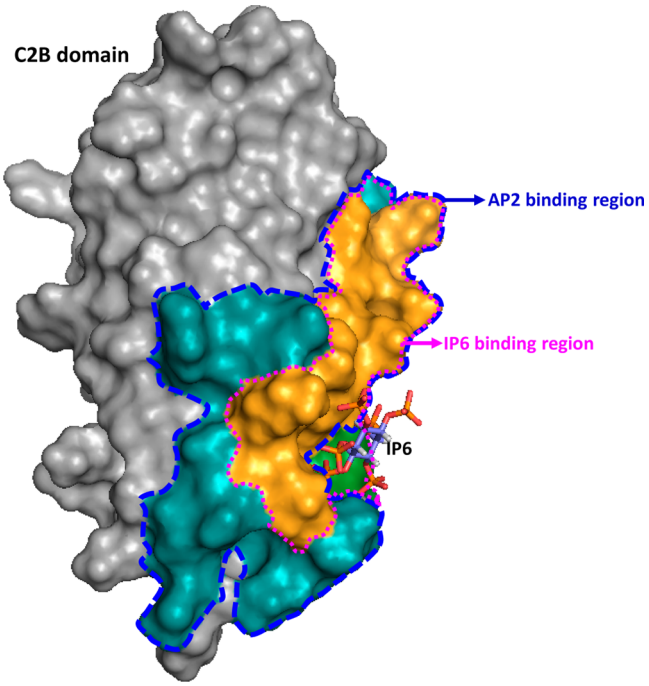

Figure 7. Surface representation of the C2B domain in the C2B−IP6 complex. The AP-2 binding region is colored cyan and orange; the IP6 binding region (perturbed region) on C2B is colored in orange and green, and IP6 is shown in ball-and-stick representation.

V376. The four intermolecular NOEs that are involved in binding to IP6 were used for the structure calculation. The 10 C2B−IP6 complex structures with the lowest energies were deposited in the PDB as entry 2LHA.

Mechanism of the Inhibition of Synaptic Vesicle Endocytosis by IP6. Mizatuni et al. reported that binding of IP6 to the C2B domain of Syt altered the Syt I−AP-2 interaction.[14] These authors generated a GST−C2B fusion protein and allowed it to interact with AP-2, followed by elution with 50 μM IP6. They then analyzed the eluent and found that AP-2 had been eluted out, indicating that IP6 competes with AP-2 for binding to the C2B domain. Furthermore, Grass et al. reported that a basic motif peptide (K321−K332) within the C2B domain was sufficient for binding to AP-2.[50] The dissociation constant for this peptide and AP-2 was in the micromolar range. This result also suggested that IP6 would be able to compete with AP-2 for binding to the C2B domain. In this study, we found that the IP6 binding site in the C2B domain is distributed in two regions (Figure 7). These regions overlap with the AP2 binding site on C2B. In the C2B−IP6 complex structure, we observed minor conformational changes in both regions. The interaction between the C2B domain and AP-2 was reported to play an important role in the endocytosis of synaptic vesicles. It was reported that IP6 plays an important role by inhibiting the interaction between AP-2 and the C2B domain of Syt I. The molecular level description of the C2B−IP6 complex structure presented here showed that the IP6 binding region overlaps with the AP-2 binding region (Figure 7). Thus, IP6 can play an important role in regulating the AP-2-mediated inhibition of neurotransmitter release that blocks endocytosis. This information will be helpful in developing better pharmaceutical treatments for neurological disorders.

■ ASSOCIATED CONTENT

Accession Codes

The molecular coordinates were deposited in the Protein Data Bank as entry 2LHA, and the NMR data were deposited in the BMRB as entry 5194.

■ AUTHOR INFORMATION

Corresponding Author

*Department of Chemistry, National Tsing Hua University, Hsinchu 30013, Taiwan. Fax: 011-886-35-711082. Phone: 011-886-35-721524. E-mail: cyu.nthu@gmail.com.

Funding

We thank the National Science Council (NSC) Taiwan (Grant NSC 100-2113-M-007-012-MY3) for financial support.

Notes

The authors declare no competing financial interest.

■ ACKNOWLEDGMENTS

We appreciated the 700 MHz Nuclear Magnetic Resonance Facility in the Chemistry Department, National Tsing Hua University.

■ ABBREVIATIONS

Syt I, synaptotagmin I; IP6, inositol hexaphosphate; NMR, nuclear magnetic resonance; HSQC, heteronuclear single-quantum coherence spectroscopy; TOCSY, total correlation spectroscopy; NOESY, nuclear Overhauser enhancement spectroscopy; ARIA, ambiguous restraints for iterative assignment; CNS, Crystallography and NMR System; rmsd, root-mean-square deviation.

■ REFERENCES

(1) Ullrich, B., Li, C., Zhang, J. Z., McMahon, H., Anderson, R. G. W., Geppert, M., and Südhof, T. C. (1994) Functional properties of multiple synaptotagmins in brain. *Neuron 13*, 1281−1291.

(2) Schiavo, G., Osborne, S. L., and Sgouros, J. G. (1998) Synaptotagmins: More isoforms than functions? *Biochem. Biophys. Res. Commun. 248*, 1−8.

(3) Perin, M. S., Fried, V. A., Mignery, G. A., Jahn, R., and Sudhof, T. C. (1990) Phospholipid binding by a synaptic vesicle protein homologous to the regulatory region of protein kinase C. *Nature 345*, 260−263.

(4) Chapman, E. R. (2008) How does synaptotagmin trigger neurotransmitter release? *Annu. Rev. Biochem. 77*, 615−641.

(5) Geppert, M., Goda, Y., Hammer, R. E., Li, C., Rosahl, T. W., Stevens, C. F., and Südhof, T. C. (1994) Synaptotagmin I: A major Ca^{2+} sensor for transmitter release at a central synapse. *Cell 79*, 717−727.

(6) Shao, X., Li, C., Fernandez, I., Zhang, X., Sudhof, T. C., and Rizo, J. (1997) Synaptotagmin-syntaxin interaction: The C2 domain as a Ca^{2+}-dependent electrostatic switch. *Neuron 18*, 133−142.

(7) Chapman, E. R., Hanson, P. I., An, S., and Jahn, R. (1995) Ca^{2+} regulates the interaction between synaptotagmin and syntaxin 1. *J. Biol. Chem. 270*, 23667−23671.

(8) Zhang, J. Z., Davletov, B. A., Sudhof, T. C., and Anderson, R. G. W. (1994) Synaptotagmin I is a high affinity receptor for clathrin AP-2: Implications for membrane recycling. *Cell 78*, 751−760.

(9) Schiavo, G., Gmachi, M. J. S., Steinbeck, G., Sollner, T. H., and Rothman, J. E. (1995) A possible docking and fusion particle for synaptic transmission. *Nature 378*, 733−736.

(10) Schiavo, G., Stenbeck, G., Rothman, J. E., and Sollner, T. H. (1997) Binding of the synaptic vesicle v-SNARE, synaptotagmin, to the plasma membrane t-SNARE. SNAP-25, can explain docked vesicles at neurotoxin-treated synapses. *Proc. Natl. Acad. Sci. U.S.A. 94*, 997−1001.

(11) Mehta, P. P., Battenberg, E., and Wilson, M. C. (1996) SNAP-25 and synaptotagmin involvement in the final Ca^{2+}-dependent triggering of neurotransmitter exocytosis. *Proc. Natl. Acad. Sci. U.S.A. 93*, 10471−10476.
(12) Sheng, Z. H., Yokoyama, C. T., and Catterall, W. A. (1997) Interaction of the synprint site of N-type Ca^{2+} channels with the C2B domain of synaptotagmin I. *Proc. Natl. Acad. Sci. U.S.A. 94*, 5405−5410.
(13) Kim, D. K., and Catterall, W. A. (1997) Ca^{2+}-dependent and -independent interactions of the isoforms of the α1A subunit of brain Ca^{2+} channels with presynaptic SNARE proteins. *Proc. Natl. Acad. Sci. U.S.A. 94*, 14782−14786.
(14) Mizutani, A., Fukuda, M., Niinobe, M., and Mikoshiba, K. (1997) Regulation of AP-2-synaptotagmin interaction by inositol high polyphosphates. *Biochem. Biophys. Res. Commun. 240*, 128−131.
(15) Fukuda, M., Aruga, J., Niinobe, M., Aimoto, S., and Mikoshiba, K. (1994) Inositol-1,3,4,5-tetrakisphosphate binding to C2B domain of IP4BP/synaptotagmin II. *J. Biol. Chem. 269*, 29206−29211.
(16) Ninobe, M., Yamaguchi, Y., Fukuda, M., and Mikoshiba, K. (1994) Synaptotagmin is an inositol polyphosphate binding protein: Isolation and characterization as an Ins 1,3,4,5-P4 binding protein. *Biochem. Biophys. Res. Commun. 205*, 1036−1042.
(17) Mehrotra, B., Elliott, J. T., Chen, J., Olszewski, J. D., Profit, A. A., Chaudhary, A., Fukuda, M., Mikoshiba, K., and Prestwich, G. D. (1997) Selective photoaffinity labeling of the inositol polyphosphate binding C2B domains of synaptotagmins. *J. Biol. Chem. 272*, 4237−4244.
(18) Mikoshiba, K., Fukuda, M., Ibata, K., Kabayama, H., and Mizutani, A. (1999) Role of synaptotagmin, a Ca^{2+} and inositol polyphosphate binding protein, in neurotransmitter release and neurite outgrowth. *Chem. Phys. Lipids 98*, 59−67.
(19) Schiavo, G., Gu, Q.-M., Prestwich, G. D., Söllner, T. H., and Rothman, J. E. (1996) Calcium-dependent switching of the specificity of phosphoinositide binding to synaptotagmin. *Proc. Natl. Acad. Sci. U.S.A. 93*, 13327−13332.
(20) Xu, Q., Kanthasamy, A. G., and Reddy, M. B. (2008) Neuroprotective effect of the natural iron chelator, phytic acid in a cell culture model of Parkinson's disease. *Toxicology 245*, 101−108.
(21) Graf, E., and Eaton, J. W. (1990) Antioxidant functions of phytic acid. *Free Radical Biol. Med. 8*, 61−69.
(22) Llinás, R., Sugimori, M., Lang, E. J., Morita, M., Fukuda, M., Niinobe, M., and Mikoshiba, K. (1994) The inositol high-polyphosphate series blocks synaptic transmission by preventing vesicular fusion: A squid giant synapse study. *Proc. Natl. Acad. Sci. U.S.A. 91*, 12990−12993.
(23) Mizutani, A., Fukuda, M., Ninobe, M., and Mikoshiba, K. (1997) Regulation of AP-2-synaptotagmin interaction by inositol high polyphosphates. *Biochem. Biophys. Res. Commun. 240*, 128−131.
(24) Goddard, T. D., and Kneller, D. G. (2008) *SPARKY 3*, University of California, San Francisco.
(25) Grzesiek, S., and Bax, A. (1992) An efficient experiment for sequential assignment of medium sized backbone isotopically enriched protein. *J. Magn. Reson., Ser. B 110*, 201−210.
(26) Wittekind, M., and Mueller, L. (1993) HNCACB, a high sensitivity 3D NMR experiment to correlate the amide proton and nitrogen resonances with α-carbon and β-carbon resonances in proteins. *J. Magn. Reson., Ser. B 99*, 638−643.
(27) Clubb, R. T., Thanabal, V., and Wagner, G. A. (1992) Constant time 3-dimensional triple resonance pulse scheme to intraresidue H-1(N), N-15, C-13′ chemical shifts in N-15, C-13 enriched proteins. *J. Magn. Reson. 97*, 213−217.
(28) Kay, L. E., Xu, G. Y., and Yamazaki, G. (1994) Enhanced-sensitivity triple-resonance spectroscopy with minimal H_2O saturation. *J. Magn. Reson., Ser. A 109*, 129−133.
(29) Pascal, S. M., Muhandiram, D. R., Yamazaki, T., Forman-Kay, J. D., and Kay, L. E. (1994) Simultaneous acquisition of ^{15}N- and ^{13}C-edited NOE spectra of proteins dissolved in H_2O. *J. Magn. Reson., Ser. B 103*, 197−201.
(30) Breeze, A. L. (2000) Isotope-filtered NMR methods for the study of biomolecular structure and interactions. *Prog. Nucl. Magn. Reson. Spectrosc. 36*, 323−372.
(31) Rieping, W., Habeck, M., Bardiaux, B., Bernard, A., Malliavin, T. E., and Nilges, M. (2007) ARIA2: Automated NOE assignment and data integration in NMR structure calculation. *Bioinformatics 23*, 381−382.
(32) Cornilescu, G., Delaglio, F., and Bax, A. (1999) Protein backbone angle restraints from searching a database for chemical shift and sequence homology. *J. Biomol. NMR 13*, 289−298.
(33) Laskowski, R. A., Rullmannn, J. A., MacArthur, M. W., Kaptein, R., and Thornton, J. M. (1996) AQUA and PROCHECK-NMR: Programs for checking the quality of protein structures solved by NMR. *J. Biomol. NMR 8*, 477−486.
(34) Dominguez, C., Boelens, R., and Alexandre, M. J. J. B. (2003) HADDOCK: A protein-protein docking approach based on biochemical and/or biophysical information. *J. Am. Chem. Soc. 125*, 1731−1737.
(35) De Vries, S. J., van Dijk, A. D. J., Krzeminski, M., van Dijk, M., Thureau, A., Hsu, V., Wassenaar, T., and Bonvin, A. M. J. J. (2007) HADDOCK versus HADDOCK: New features and performance of HADDOCK2.0 on the CAPRI targets. *Proteins: Struct., Funct., Bioinf. 69*, 726−733.
(36) Veverka, V., Crabbe, C., Bird, I., Lennie, G., Muskett, F. W., Taylor, R. J., and Carr, M. D. (2008) Structural characterization of the interaction of mTOR with phosphatidic acid and a novel class of inhibitor: Compelling evidence for a central role of theFRB domain in small molecule-mediated regulation of mTOR. *Oncogene 27*, 585−595.
(37) Tomaselli, S., Ragona, L., Zetta, L., Assfalg, M., Ferranti, P., Longhi, R., Bonvin, A. M. J. J., and Molinari, H. (2007) NMR-based modeling and binding studies of a ternary complex between chicken liver bile acid binding protein and bile acids. *Proteins: Struct., Funct., Bioinf. 69*, 177−191.
(38) Brunger, A. T., Adams, P. D., Clore, G. M., Delano, W. L., Gros, P., Grosse-Kunstleve, R. W., Jiang, J.-S., Kuszewski, J., Nilges, M., Pannu, N. S., Read, R. J., Rice, L. M., Simonson, T., and Warren, G. L. (1998) Crystallography & NMR system: A new software system for macromolecular structure determination. *Acta Crystallogr. D54*, 905−921.
(39) Petros, M., Kawai, M., Luly, J. R., and Fesik, S. W. (1992) Conformation of two non-immunosuppressive FK506 analogs when bound to FKBP by isotope-filtered NMR. *FEBS Lett. 308*, 309−314.
(40) Kleywegt, G. J. (2007) Crystallographic refinement of ligand complexes. *Acta Crystallogr. 63*, 94−100.
(41) Hubbard, S. J., and Thornton, J. M. (1993) *NACCESS*, University College London, London.
(42) Jorgenson, W. L., and Tirado-Rives, J. (1988) The OPLS (optimized potentials for liquid simulations) potential functions for proteins, energy minimizations for crystals of cyclic peptides and crambin. *J. Am. Chem. Soc. 110*, 1657−1666.
(43) Fernandez-Chacon, R., Konigstorfer, A., Gerber, S. H., Garcia, J., Matos, M. F., Stevens, C. F., Brose, N., Rizo, J., Rosenmund, C., and Sudhof, T. C. (2001) Synaptotagmin I functions as a calcium regulator of release probability. *Nature 410*, 41−49.
(44) Maximov, A., and Sudhof, T. C. (2005) Autonomous function of synaptotagmin 1 in triggering synchronous release independent of asynchronous release. *Neuron 48*, 547−554.
(45) Mochida, S., Fukuda, M., Niinobe, M., Kobayashi, H., and Mikoshiba, K. (1997) Roles of synaptotagmin C2 domains in neurotransmitter secretion and inositol high-polyphosphate binding at mammalian cholinergic synapses. *Neuroscience 77*, 937−943.
(46) Fukuda, M., and Mikoshiba, K. (1997) The function of inositol high polyphosphate binding proteins. *BioEssays 19*, 593−603.
(47) Pierce, M. M., Raman, C. S., and Nall, B. T. (1999) Isothermal titration calorimetry of protein-protein interactions. *Methods 19*, 213−221.
(48) Chang, Y. G., Song, A. X., Gao, Y. G., Shi, Y. H., Lin, X. J., Cao, X. T., Lin, D. H., and Hu, H. Y. (2006) Solution structure of the

ubiquitin-associated domain of human BMSC-UbP and its complex with ubiquitin. *Protein Sci. 15*, 1248−1259.
(49) Fukuda, M., Kojima, T., Aruga, J., Niinobe, M., and Mikoshiba, K. (1995) Functional diversity of C2 domains of synaptotagmin family. Mutational analysis of inositol high polyphosphate binding domain. *J. Biol. Chem. 270*, 26523−26527.
(50) Grass, I., Thiel, S., Honing, S., and Haucke, V. (2004) Recognition of a Basic AP-2 Binding Motif within the C2B Domain of Synaptotagmin Is Dependent on Multimerization. *J. Biol. Chem. 279*, 54872−54880.